

DESIGN AND INTEGRATION OF A DEPLOYABLE ANTENNA WING ASSEMBLY

Edward A. Boesiger⁽¹⁾, Garrett Cullen⁽¹⁾, Will Johnston⁽²⁾

⁽¹⁾ Lockheed Martin Space, 1111 Lockheed Martin Way, Sunnyvale, CA 94089 USA

⁽²⁾ Lockheed Martin Space, 12257 South Wadsworth Boulevard, Littleton, CO 80127 USA
ed.boesiger@lmco.com, garrett.m.cullen@lmco.com, will.m.johnston@lmco.com

ABSTRACT

As one combines mechanisms into a larger deployable subassembly, there are things to consider and of course, lessons to be learned. This Antenna Wing Assembly was designed mostly with components that had been flown previously but that did not prevent surprises during integration and test.

OVERALL DESIGN DESCRIPTION

This Antenna Wing Assembly (AWA) deploys two communication antennas away from the spacecraft (Fig. 1). The AWA consists of a hinge line that deploys the assembly 90 degrees after release, with a flexible section of waveguide across the joint and a spool to contain and guide the harness. The hinges are damped Neg'ator spring-driven, duplex-bearing hinges with a cam latch. An aluminum honeycomb/M55J composite structure holds two two-axis gimbal antenna assemblies. The gimbals are a common product used on multiple spacecraft so to carry these particular RF frequencies, an external rotary waveguide joint (RWJ) was used to transfer the signals across. The dual band antenna was also a reuse from a previous program. Restraint to the spacecraft during launch is provided by eight low-shock split spool release devices, also a common product used on many Lockheed Martin spacecraft. These were particularly arranged to ensure the loads into the standard product hinges, antennas, and gimbals were enveloped by previous qualification testing.

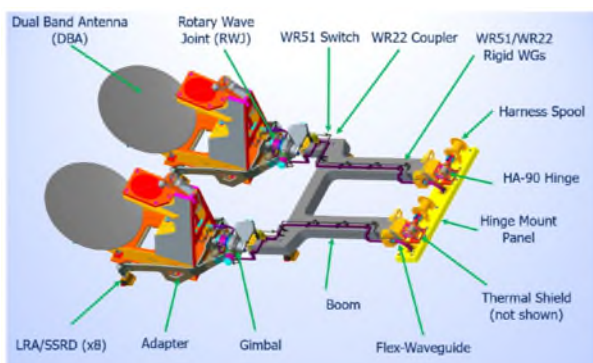


Figure 1. Antenna Wing Assembly components

Hinge line Alignment

Note that each of the hinges on the hinge line had duplex bearings so alignment of these hinges was critical to prevent binding. To help ensure alignment, they were attached to a composite mount panel (Fig. 2). The structure included some designed-in compliance to allow small (<0.25 mm (0.010 inch)) hinge-to-hinge misalignment.

The hinges are set 53 cm (21 in) apart. Using photogrammetry, the deployed hinge's inboard planes are measured along with the hinge mount panel's inserts plane. Solid stainless-steel custom shims were machined and installed between the hinge's clevis and the mount panel to provide a stress-free inboard clevis mounting surface. In practice, the mounting panel was sufficiently flat such that shims were not needed to ensure the correct alignment of the hinge axes; therefore, they were not included in the flight build. The hinge fasteners were then secured with bonded, load-bearing washers to complete the installation.

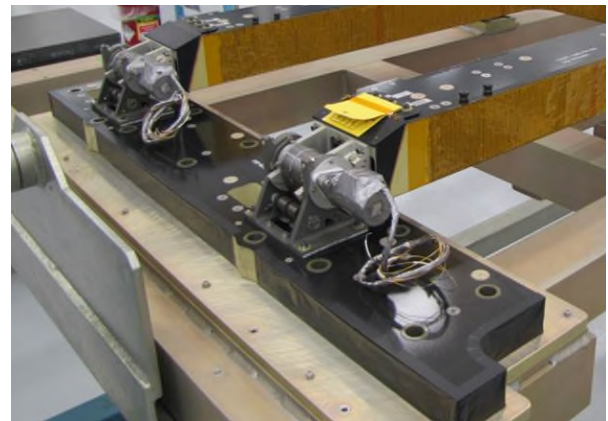


Figure 2. Hinges attached to mount panel

On a past program, a similar antenna wing was designed as an integral part of the spacecraft structure. That approach required the wing to be delivered early in spacecraft single-line flow for modest savings in the cost of a single structural panel. By deliberately including a base panel for the hinges and by designing all harnesses and release devices to be independent from the spacecraft, the AWA was fully modular and could be

removed or installed without impacting the spacecraft. By designing for modularity from the outset, the AWA had additional time for component design, manufacturing, and testing.

Composite Life

In this application, the strength and stiffness of the composite structure was important to be maintained throughout the mission, not just during launch. Recent test data on composites has shown that structures can fatigue with thermal cycling (in this case expected to be about 5000 cycles). This cyclic failure is driven by the mismatch in coefficients of thermal expansion between the aluminum core and graphite composite facesheets. As the panels are repeatedly thermal cycled, small voids begin to form, which expand. These voids allow the facesheets to separate from the core under significantly less load than at the beginning of life. The primary contributions to this delamination are the number of cycles and the temperature range of each cycle, though the behavior also depends on the material and geometry of the structure. The composite structure analysis included end of life consideration for stiffness and strength degradation. Testing could have answered the questions above concerning end of life strength and stiffness but would have taken prohibitively long by the time the need was documented. Because adequate margins were expected, a worst-case analysis approach was pursued instead of testing. A worst-case, finite-element model was developed to characterize the strength and stiffness of the AWA structures even with complete separation of the composite facesheets from the aluminum honeycomb core. The results were then compared to the requirements to evaluate the worst-case margin and all were shown to be acceptable.

Gimbal Design and Margins

There are many options on how to actually move the antennas – and one was a previously used steerable antenna pointing mechanism (SAPM). The SAPM is a swash-plate design with flexures, using a stepper motor actuator driving a lead screw and a linkage. The SAPM has the advantages of being compact, but it has additional complexities in aligning the axes orthogonal and challenging thermal blankets needed to protect the mechanism. The common product gimbal is comparable in terms of mass and volume and is comprised of simple, cylindrical geometry that could be directly covered by thermal coatings rather than requiring a moving blanket. Finally, orthogonality of the gimbal axes is trivial to control through machining tolerances of the connecting bracket. The common gimbal worked without issue on the AWA throughout manufacturing and testing.

The gimbals are composed of two actuators that each contain a stepper motor, harmonic drive and potentiometers. Per AIAA S-114A-2020, a step stability

analysis using MATLAB was conducted. This was a Monte Carlo simulation, varying 21 motor and drive parameters. Each parameter was assigned a distribution type (normal, uniform, or binary for the step rate parameter) and minimum and maximum values for each parameter were assigned from either the gimbal specification, actual test data, or estimated by experience. The model was run for 1000 randomly generated cases to show that step integrity was maintained.

The model was then used to calculate torque margin. Motor parameters were set to nominal values and the external drag torque was increased until the model lost stability. This validated that the model would go unstable with high drag. The drag was then set to twice the measured amount to demonstrate 100% margin and a Monte Carlo analysis performed to show that the system maintained integrity.

COMPONENT TESTING

Some testing had to be done at component level for many reasons. It reduces schedule risk for long lead time items, ensuring those items will function properly once integrated into the AWA (e.g., hinges, gimbals, rotary waveguide). Others are life tested and thus needed separate test from flight unit (e.g., harness). Some items are difficult to test due to configuration or much easier to obtain specialized data at component level (e.g., structure, antenna).

The previously qualified antenna, release device, hinges and gimbals were subjected to acceptance testing at component level. It was initially thought that acceptance testing would be all that was needed for the flexible waveguide that crosses the hinge line. However, thermal predicts showed that the qualification temperatures were being exceeded. The 12-year-old qual unit was found and determined that it was stored properly such that additional testing could be ‘added’ to the qualification. Pressure leak, VSWR (voltage standing wave ratio), thermal cycles and a deployment test were done to extend the hot survival temperature capability range from 125°C to 140°C and operational from 71°C to 85°C.

Each part of the AWA structure – antenna mounting, boom, hinge mount – was tested to protoqual levels (less than qualification, more than acceptance such that the unit remains a viable flight unit). There were coupon tests and then the flight units were subjected to 15 thermal cycles (-66°C to 95°C) and static load tests at the structure supplier.

Both the harness configuration that crosses the hinge line and the configuration that crosses the gimbal axes were tested for continuity, resisting torque vs angle at temperature, and life. A simple fixture of 80/20 aluminum (Fig. 3) was connected to a load cell and motor

to cycle the harness. The life test was done at acceptance temperatures for 7000 cycles (1.5x life).



Figure 3. Hinge harness life test set up

RWJ Qualification

A rotary waveguide using ball bearings is used to carry the signals across the two-axis gimbal (Fig. 4). That mechanism was also subjected to vibration, thermal vac, RF, and life tests on a qualification unit.

This seemingly simple rotary waveguide proved to be challenging. It is self-aligning with the waveguides but only to a point, and due to misalignment tolerances, loads are present in these small bearings. Additionally, temperatures can reach -85°C to $+95^{\circ}\text{C}$, and when the mechanism is incorporated with waveguide runs these thermal extremes create external loading due to the expansion and contraction of the runs. Unfortunately, the life test was done without these external loads, and only tested the life capability under the effects of preload and temperature (i.e., internal effects of temperature on preload). To validate life and on-orbit performance, a cumulative fatigue damage assessment was done between the life test conditions (7000 cycles at 1138 MPa (165 ksi) average stress) and the average flight conditions (about 5000 cycles at 1069 MPa (155 ksi) average stress) to show acceptable margins.

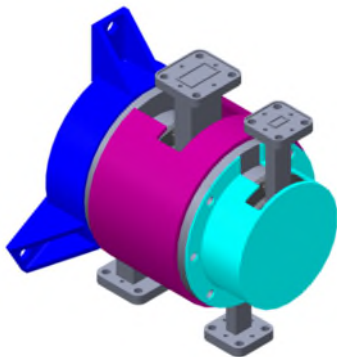


Figure 4. Solid model of the Rotary Waveguide Joint

The cumulative fatigue analysis had to be redone later as

it was found that when the gimbal and RWJ were mated, the axes of rotation were defined by probing the housing cylinder of the RWJ and the gimbal mounting flanges rather than characterizing the rotational axes through motion tracking as is typically done. This produces uncertainty in the alignment as an axis defined by such external features may not be the functional rotational center. Due to tolerances like bearing runout and diametrical positional tolerances of the features to the bearing center, the actual misalignment may, therefore, be more than the specified allowable of 0.13 mm (0.005 in) which was assumed for the fatigue analysis. A review of the applicable tolerances of the involved drawings revealed that the misalignment could be almost twice the originally specified amount. Fortunately, the load increase was low enough to maintain all required margins.

Sunshield Addition

Late in the design cycle, thermal analysts indicated that there was a spacecraft orientation that would heat the hinges to unacceptable temperatures. A sunshield was designed and tested for its torque resistance (it actually helps deployment) and life. The assisting torque was a key design driver to prevent torque margin erosion late in the design process. The sunshield is black Kapton[®] stretched between lenticular struts that are passively released with the AWA. It fits within the 6.4 cm (2.5 in) clearance between the boom and panel.

The harness test stand was modified to accept the sunshield in order to perform torque and life testing at operational and survival temperatures. It was tested for 100 cycles (same as hinges and flex-waveguides).

Development testing the sunshield revealed several design shortcomings, which were resolved in the flight design (which of course is why development testing is done and is so valuable). The multilayer Kapton[®] blanket was initially built using standard blanket processes, including edges taped with pressure-sensitive adhesive. When this tape was folded to follow the lenticular struts, it creased and bent at a single point that required additional input torque. For flight, this creasing was mitigated by eliminating the edge tape in the folding regions, which allowed the Kapton[®] layers to slide past each other with minimal resistance.

A further segment of tape was initially applied over the edges of the lenticular strut to prevent abrasion of the blanket. Troubleshooting showed this tape to create a stick-slip phenomenon as the tape stiffened at colder temperatures. The effect was negligible at 20°C and it gradually increased when observed at 5°C increments down to -10°C . For flight, this tape was eliminated and no adverse wear was observed on the blanket during life testing. Note that the glass transition temperature of

many common pressure-sensitive adhesives is around -10°C, so tapes quickly become significantly stiffer at cold temperatures.

During development testing, the sunshield blanket was secured in the center of one side of the blanket. At the cold temperature extreme this single tie-down point caused the blanket to bend and release at the same deployment angle as a stick-slip phenomenon was observed in the torque data. The single restraint was replaced by two restraints, each of which was in line with the respective lenticular spring, eliminating a “beam” of tape that could bend when cold. Shorting out this tape and its associated adhesive served to increase the available torque of the sunshield mechanism, further demonstrating the importance of eliminating any adhesives in the moving portion of a multilayer thermal blanket. When possible, avoid designing any blanket that must move, but if moving blankets are necessary, take care to eliminate adhesives in the moving regions.

AWA ASSEMBLY AND TEST

Boom Deployment

Once the hinges and boom are assembled, they are deployed multiple times to demonstrate the integrated mechanism. Stowing the hinges for a deployment requires that the spring-loaded cam latches be retracted and restrained.

To stow the AWA is a manual operation and with a large deployable, that means a large moment arm. Care is taken to not go too quickly such as to not overload the damper. For one such stowing, the latches were inadequately restrained and one of the latches caught on the cam track and damaged the hinge, as shown in Fig. 5. This damaged hinge was replaced with a spare, and the remaining hardware was exonerated. When stowing mechanisms with spring-loaded latches, and especially ones where a large moment arm can cause high forces, appropriate tooling is recommended.

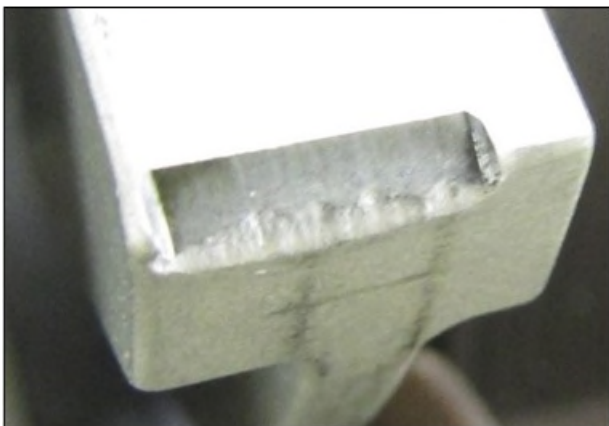


Figure 5. Hinge latch cam track after damage

Harnesses

The harnesses have tightly wrapped copper tape that extends approximately 18 cm (7 in) beyond the connector face (Fig. 6). Extensive harness shielding is required for harnesses outside the spacecraft due to the mission’s stringent EMI requirements. This made the harness so stiff that it prevented the harness from being routed around waveguide and structure.

The solution was to cut off the connector, adjust the harness length to optimize routing, re-attach connector, re-form the harness with the required tight bends, and re-wrap the harness with tape and germanium Kapton® tube. The main issue with this harness build was that it was done on a flat pattern and not on a 3D formboard. To compress the rework schedule, the harnesses were reworked on the flight structure, causing a significant delay to the overall assembly. Anytime harnesses are wrapped they should be built on a 3D formboard so that they can be formed and wrapped in the correct length and shape.



Figure 6. Copper wrapping made the harness very stiff

Routing the moving harnesses around the two-axis gimbals posed a particular challenge. These harnesses need to clear numerous critical interfaces without contact, and they must be routed to minimize resisting torque against the gimbals. In order to ensure adequate clearances at all gimbal positions, the harnesses were re-routed during gimbal range of motion testing. The routing could have been simplified if harness-level torque testing had been performed with a greater range of harness lengths – but of course that is atypical due to the expense of multiple harness builds.

Waveguides

As seen back in Fig.1, the waveguides are mounted to the boom and then are routed around the gimbal to the antenna. During AWA assembly, a waveguide was seen to be bent, with root cause surmised to be that it was somehow bumped by a tool or human with a small force (maybe 22 N (5 lb)). That waveguides can be damaged by a small force is not a surprise as they are not known to be robust.

The root cause investigation led to the realization that due to brazing methods used during the waveguide assembly, the copper waveguide may become fully annealed (silver solder melts at 620°C, copper anneals at 400°C). The waveguides are made with UNS C10200 copper, 99.95% pure copper, oxygen and hydrogen free; basically, what is used in wire.

With the copper guides mounted on a composite panel, the thermal strains induce loads, especially at bends. At the cold temperatures predicted the copper shrinks relative to the composite structure. The structure stretches the copper overall and while tensile stress is not bad, the local loading at the cast-in corner fittings causes high tensile stress near the “L” bend (Fig.7).

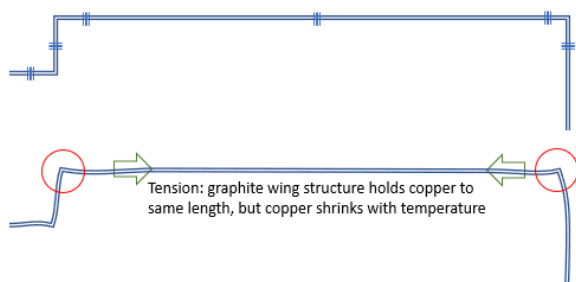


Figure 7. Thermal loads on waveguide

Materials tests were done on the removed bent waveguide and showed Knoop hardness consistent with annealed copper. Using a value of 27 MPa (4 ksi) yield strength, the analysis predicts yield or borderline yield. If the waveguide does yield, the predicted permanent set was 25 μm to 150 μm (0.001 to 0.006 inch) maximum. With the hardware built, and the waveguides being a very long lead item, the thought was maybe a little yield on orbit will not matter. But what was unknown was the impact on RF performance if yield did occur.

Additional testing was required to show positive stress margin. To provide confidence in the stress allowable, several units needed to be tested. The spare unit was needed to replace the bent one. Luckily, two other units had been delivered but were scrapped due to being out of dimensional tolerance and had not been destroyed. These units were of the same lot of product so provided good material data and were and tested. This resulted in a slight positive margin above yield (3%). A further set of tests was later performed on spare replacement parts, which confirmed the material properties of the fully annealed waveguides, which rapidly work-hardened as they were pulled to 0.2% engineering yield. Where purposefully done, yielding was highly plastic with no cracking or crippling. Furthermore, RF testing was performed before and after yield testing the second set of samples, which demonstrated that any change in RF performance was smaller than the calibration uncertainty of the measurements. The RF team looked at the results and

determined that with slight positive margin, what these samples looked like after testing, and the RF performance of the deformed samples, the waveguides were acceptable.

EMI

Heaters were required on the composite structure – which is not typical as most structure is, or is close to, the spacecraft bus. Silver-filled epoxy was initially chosen for sealing the EMI protective layers of the heaters, but was later scrutinized due to CTE mismatch concerns considering the thermal environments to be encountered. An LN₂ dunk test was done to try to efficiently validate the design. The combination (silver-filled epoxy bonded to composite panel) failed the coupon LN₂ dunk test in cohesion, with adhesion passing. Some compromises had to be made and a silicone adhesive was used instead to provide some compliance between the bond under thermal extremes. However, the silicone adhesive creates a less conductive bond and exceptions to EMI grounding requirements had to be taken. The change to silicone adhesive also negatively impacted schedule due to increased cure times. The layered nature of the EMI sealing required that full cure be achieved at each step before proceeding for outgassing reasons. This meant a 10-day cure between layers rather than the 48 hours of the silver filled epoxy. To mitigate the increased cure time, additional coupons were created as a full mock-up of the EMI seal with handling cure times only. The coupons were monitored and evaluated for any signs of outgassing issues (e.g., bubbling under tapes). Through this testing the cure time was successfully reduced to 24 hours between layers (i.e., handling cure only).

Gimbal Drive Electronics

Driving flight motors and reading telemetry from them can require complex electrical ground support equipment (EGSE) consoles. This task is complicated by driving multiple gimbal axes, primary and redundant motors, all while collecting multiple channels of telemetry. Furthermore, software is needed to correlate position to telemetry readings. For the AWA, it was determined that all of the required electronics were already available and all test requirements could be met by connecting these components with a specially designed set of nonflight harnesses. The EGSE was greatly simplified by switching between different connectors on the nonflight harness. The telemetry was checked using an off-the-shelf data acquisition system that was calibrated using a nonflight gimbal ahead of AWA testing..

Sunshield Installation

The deployable sunshield has brackets that need to be aligned parallel to each other to prevent twisting of the springs. During development testing, it was observed that misaligning the lenticular support brackets more than 0.8

mm (.03 in) caused the springs to twist, which correspondingly reduced the deployment torque provided by the mechanism. Multiple configurations of alignment tools were considered to adequately restrain the springs and to provide sufficient clearance for tooling. These designs were tested in a virtual reality simulation, showing realistic ergonomic access for the tools used to install the hardware.

Based on inspection reports, it was noted that the parts came in well within tolerance, and significant adjustments of the hardware would not be necessary. Instead of using cumbersome tooling, the hardware was installed by biasing the support brackets towards the same side of the interface holes in two directions. This approach was verified using precision photogrammetry measurements, which could be performed iteratively with small adjustments to the brackets. The process of biasing the brackets in the holes worked so well, that no adjustments were needed to meet the installation tolerances, and the parts were installed quickly and without issue.

Launch Restraints

The Launch Restraint Assembly (LRA) consists of a split spool release device (SSRD), conical shear ties, a retraction spring to pull the preload rod, and a honeycomb absorber to reduce shock from rod retraction. These assemblies had been used on multiple prior spacecraft for similar applications. The SSRDs are refurbishable, not resettable, so to ensure flight integrity they are required to go back to the supplier for rebuild and retest – which takes time and money. Since there are eight tie down points per AWA, in the effort to save both time and money, it was proposed to only do a true SSRD-driven release test on the space vehicle after acoustic test and none at AWA level. That idea was modified in two ways.

The deployment test at the AWA level was to get a baseline deployment time and generally check clearances. Generated shock data is not required at the AWA level and is collected at spacecraft-level testing as that is the most accurate conditions for shock. Instead of all eight LRAs to release the AWA, only two were used. The two LRA locations on the boom represent the worst case for deployment as those were in the deepest cavity, closest to the hinge line and thus smallest departure angle (tightest clearance). Furthermore, these are the final LRAs released on-orbit, providing a flight-like release.

Even though the other six LRA locations were not used for the deployment test, a check was done that the LRA could be installed at those other positions. The thought was to avoid installing the LRAs for the very first time on this new design at the space vehicle level where time is even more precious.

The practice installation check proved to be invaluable. Overall, it resulted in eight drawings needing updates to correct errors and provide clearer direction, the strain gage measurement equipment calibration procedure needed to be modified, the inspection plan updated, and new tools needed for ergonomics and configuration. Actually, in two locations, the LRAs were impossible to install (Fig. 8). New tooling was absolutely needed, but the AWA needed to continue processing toward installation on the vehicle. The new tools were designed and then the technicians used the Lockheed Martin virtual reality center to practice and complete the design. Virtual reality allowed the geographically isolated design, tooling, and manufacturing teams to collaborate closely on the design changes despite pandemic-related restrictions on in-person meetings. The next installation on the vehicle was successful.



Figure 8. Difficult access – a person who has four hands would be helpful!

Even with improved tooling, access to the launch restraint assemblies remained a challenge. Early in the design phase, the LRA was optimized to maximize similarity to heritage and to minimize its size, but these two features came at the expense of the assembly being more difficult to install. Over the course of four installations to the spacecraft, multiple nuts and restraint rods were damaged when tools slipped off the small nut. Adequate spares were available to replace these damaged parts, but this demonstrates how critical it is to have integration reviews early in the design process to ensure designs consider assembly, integration, and test.

Thermal Vac Test

It was originally thought that the AWA did not require any thermal vac testing at the AWA level. The key mechanism items that are vacuum sensitive (gimbals, hinges, RWJ) are tested in vacuum and other components such as the antenna and structure are tested at operational temperatures without vacuum. However, there was still the bit of doubt with the plan as the AWA is not on the spacecraft during spacecraft TVAC due to chamber size

limitations, and the interaction of the waveguide with the composite structure, bonding, and adhesives with extreme temperatures and vacuum would not be tested prior to being on orbit. A thermal vacuum exposure test was thus planned.

After ambient deployment, prior to antenna range testing, the AWA was cycled to temperature extremes in a TVAC chamber. During assembly and test, the AWA is attached to a strongback (seen in the background of Fig. 9) and would be on this strongback with the hinges deployed while in the TVAC chamber. The release devices were uninstalled to ensure no interaction between the aluminum strongback and the composite structure.



Figure 9. AWA on assembly fixture

Since TVAC was done at AWA level, there were compromises on temperatures as one could not exceed protoqual temperature of any component (there was no qual unit; only a protoqual first unit that would fly). As stated before, many components had been tested before installation, so the compromise to the items going through test for the first time was about 10°C on each extreme. The flight heaters were powered as required to maintain thermal control. RF absorbers were placed in front of each antenna to prevent inadvertent heating of the assembly during the test. Besides temperature, the only other data collected during the test were return loss measurements for each antenna channel and the resistances of the gimbal windings and potentiometers. As expected, the non-flight waveguide segments between the AWA and the network analyzer increased the return loss in the system. Therefore, the return loss was checked for changes rather than absolute values.

Prior to TVAC testing, the launch restraint interfaces were intentionally loosened to avoid inducing thermal

expansion loads into the flight structure. After TVAC testing, photogrammetry measurements showed that the loosened interfaces had shifted during the test, so they could not be accurately measured to the hinge panel. Without this data, it was time consuming to manually center and install the LRAs when mating the AWA to the spacecraft. By measuring the LRA locations prior to TVAC, the follow-on build aligned the LRAs ahead of installation, saving time at spacecraft-level.

Antenna Range Test

After TVAC, the integrated antennas' RF performance was characterized. Because the impact of thermal blankets and support structure were believed to have a minimal impact on AWA-level RF performance, the AWA specification directly referenced the lower-level antenna performance requirements without allocating additional margin beyond waveguide losses. However, when the antennas were tested on the AWA, it was observed that the axial ratio and beam alignment shifted slightly from marginally compliant to noncompliant. These changes were shown to be acceptable at the system-level, but future designs should better define the thermal blanket configuration and should allocate additional margin for integrated antennas to pre-empt nonconformances.

VEHICLE TESTS

Vehicle-Level RF Check

The original plan was to have the AWA tested at the subsystem level with an acoustic test followed by antenna range RF testing. As the schedule kept slipping, and the AWA was needed to be installed on the vehicle for the vehicle-level acoustic test, the decision was made to streamline the test plan and skip the AWA-level acoustic test as it would be tested at vehicle and it was felt there was little risk of failures.

There was one 'hole' in that streamlined plan that was realized a few weeks before vehicle installation. Post vehicle acoustic there is a deployment of the AWA while on the spacecraft, and a range of motion test of the gimbals. This would show that the launch restraints, hinges and gimbals all survived acoustic test and are ready for launch. There was also a test of the RF function of the antenna using electrical ground support equipment (EGSE). This test could be performed as intended through the downlink switch. However, that EGSE connected through a coupler and would not test the uplink from the antenna to the coupler. With this first-time usage and design, the requirement was to ensure the entire subsystem was in working order post acoustic.

Clearly, one method of ensuring the AWA survived acoustic for both uplink and downlink was to remove the AWA from the spacecraft and re-test in the antenna

range. That was undesirable for breaking configuration with the spacecraft and the time and expense to do that test. During brainstorming sessions to find a solution, it was noted that there was a section of waveguide close to the hinge (inboard of the coupler) that may be easy to remove and replace. That remove/replace was practiced on the AWA before spacecraft installation and it actually was easy. Fig. 10 illustrates what that then enabled. Before and after acoustic test, a signal analyzer can be used where that waveguide section was removed – this shows uplink is good from antenna to spacecraft minus the removed section. When the waveguide section is then replaced, the EGSE at the switch can then check the complete downlink, and the uplink from the switch, through the now replaced waveguide section to the spacecraft.

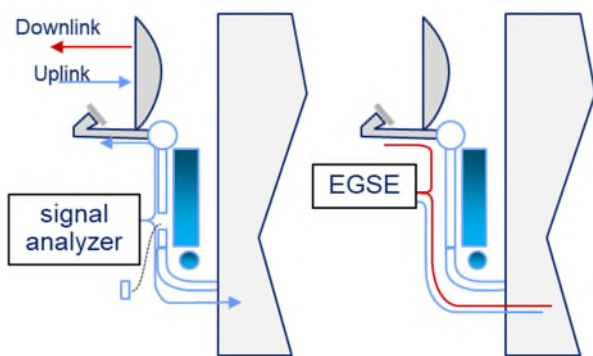


Figure 10. Testing the RF post acoustic test

It was noted during final stow of the AWA that the primary side of the gimbal potentiometer showed no signal – the deadband aligned perfectly with the stowed position. This would mean that the gimbal position would not be known after launch - however, the design ensured the redundant deadband was in a different orientation. One more aspect to check was that spacecraft computer read and reported the redundant position at all times, especially just after launch, and it did.

Offload Friction

As a part of the installation process, the AWA was deployed to demonstrate the functional performance of the mechanism. This deployment was performed on a newly installed deployment rail system that had not been used for a similar mechanism before. The same counterbalance offload as AWA-level testing (Fig. 9) was installed on this new deployment rail. Initial calculations for torque margin with an estimated friction value showed the offload system would be adequate. When the AWA was released, it deployed 80 degrees before failing to lock out (as is usually the case when these things happen, it was late in the day on a weekend!).

After reviewing the deployment rail design, it was determined that the two degree-of-freedom rails had higher friction, especially in the lateral direction, which

the AWA must traverse at the end of travel when the spring force is lowest. This friction was substantial enough that the top of the support cable would visibly lag behind the flight hardware. Friction-reducing vibrators are on the rails but were not activated as it was thought they would not be needed in this case with a simple 90 degree deployment. In order to correct for the high friction, support wires were used on subsequent deployments to manually free the stuck offload cables and keep them from slowing the deployment.

Gimbal Drive Software

The gimbal range of motion test was repeated at the spacecraft as a final verification of the mechanism clearances and as a demonstration of the spacecraft's ability to command the gimbals. The latter identified shortcomings in the gimbal command software.

Integrated testing revealed the selection of the primary motor was hard coded into the software. After the software was revised, the AWA was deployed an additional time, and the full system was successfully validated.

SUMMARY

When designing and integrating a larger deployable subsystem, the mechanism engineer needs to consider and have knowledge not only about the usual mechanism parts such as bearings, actuators, and release devices but also possibly such parts as structure, waveguides, and antennas. This Antenna Wing Assembly development provided several lessons that the team learned quickly as the second AWA build went very smoothly. The fully blanketed AWA is shown installed on the spacecraft in Fig. 11. The AWA was successfully deployed on orbit.



Figure 11. AWA installed on side of spacecraft